A Spatial Sensitivity Analysis of a Spatially Explicit Model for Myxomatosis in Belgium

Jan M. Baetens(✉) and Bernard De Baets

KERMIT, Department of Mathematical Modelling, Statistics and Bioinformatics, Ghent University, Coupure links 653, Ghent, Belgium
{jan.baetens,bernard.debaets}@ugent.be

Abstract. Motivated by their ability to mimic complex biological and natural processes, many spatially explicit models (SEMs) have been proposed during the last two decades for simulating such processes. Yet, a sensitivity analysis (SA) of such models is typically not performed, or model sensitivity is only studied over time on the basis of aggregated quantities, due to the lack of an appropriate framework. Taking a SEM for myxomatosis among European rabbits in Belgium as a model SEM, we conduct a spatial SA and investigate to what extent the sensitivity of this model varies spatially and whether or not this should become common practice when developing a SEM.

1 Introduction

Even though a sensitivity analysis (SA) is considered as a crucial step in the mathematical model development cycle [23,24], this step is often overlooked when it comes to the construction of spatially explicit models (SEMs) [12], like cellular automata (CAs) [29] and agent-based models (ABMs) [8]. The main reason for this lies in the fact that the spatial structure of such models cannot be neglected when analysing their sensitivity with respect to their inputs and parameters, whereas only very recently the first steps have been taken towards a theoretical underpinning of so-called spatial SAs [11,12,22]. Indeed, when referring to a SA in the field of SEMs, one typically means a study of how one or more aggregated quantities are affected by the SEM's inputs and/or parameters [15,17,20,27]. Still, it is to be expected that the sensitivity of such models is not necessarily spatially homogeneous, especially in the case of spatially heterogeneous inputs and/or parameters. Hence, for instance, the plausible range of model outputs might vary spatially, and likewise, different inputs and/or parameters might be the most important in different regions of the spatial domain. From a practical point of view, this implies that a small perturbation of a SEM's parameters might lead to considerable changes in the model outputs at some location, whereas these might be negligible elsewhere.

There are two main approaches two SAs of mathematical models, referred to as local and global SAs, respectively [23]. The former aims at quantifying the change in model outputs due to small perturbations of model inputs and/or

S. El Yacoubi et al. (Eds.): ACRI 2016, LNCS 9863, pp. 91–100, 2016.
DOI: 10.1007/978-3-319-44365-2_9

parameters, which is done by evaluating finite differences at specific points in the space of model inputs and/or parameters. Hence, the outcome of the SA might depend on the selected points in the parameter space. The most common method is the so-called one-at-a-time approach (OAT) in which one model input or parameter is perturbed at a time and the effect of this perturbation is determined [30]. Typically, the model input or parameter is changed with a given amount [15,20], but there are also studies where, for instance, a varying proportion of cells is swapped [6]. The main advantages of a local SA are that it is very intuitive and simple, while it is also computationally very efficient [11]. Besides, it works well when the plausible range of model inputs and/or parameters is known [7]. A global SA, on the other hand, is more comprehensive because it considers the full meaningful range of model inputs and/or parameters. As opposed to its local counterpart, these are varied simultaneously in order to quantify the interactions among them. Among the global SA methods, many trace back to Sobol's [26], or are extensions and variations thereof [25,28]. They are variance-based in that they decompose the variance of the model prediction into partial variances that represent the share in the total variance that is explained by the different model inputs and/or parameters. Only recently, Sobol's method has been extended to a spatial context [11,12]. For a more comprehensive overview of global SA methods, we refer the reader to [24].

The field of infectious disease modelling is one of the fields that has even not yet embraced non-spatial SA methods like Sobol's [26], let alone spatial SAs [31]. This is surprising because it can give insight into the plausible range of model outputs, while it can also help to allocate resources to follow-up experimentation and field study, to identify redundant parameters, and to determine the robustness of a modelling study's qualitative conclusions [2,18,24]. Furthermore, in the context of infectious disease modelling, it can help to identify those regions in the study areas where the simulation results are relatively robust, and hence where the required (human) resources and disease impacts can be estimated relatively reliably, irrespective of the uncertainty that might be involved in the model inputs and/or parameters.

Starting from an extension of the leading model simulating the spread of myxomatosis among European rabbits (*Oryctolagus cuniculus*) [3] to a spatially explicit context, we conduct a local spatial SA in order to quantify its robustness with respect to perturbations of the model parameters. We take myxomatosis as an exemplary infectious disease, because it has been well documented and the introduction of similar non-endemic epizootics is something that occurs increasingly often due to the ongoing globalization [14]. In Sect. 2 we present some basic facts on myxomatosis in general, and the epidemic wave that will be mimicked more in particular, after which we introduce the SEM for myxomatosis among European rabbits. The experimental setup is outlined in Sect. 3, while the results and conclusions of our study are presented in Sect. 4.

2 In Situ and in Silico Myxomatosis

2.1 Facts and Figures

Myxomatosis is caused by the myxoma virus that was released illegally in France in 1952 [4], after which it spread through Europe and decimated the endemic rabbit populations. In Belgium, the first cases were confirmed by the first half of September in several towns in the Northwest of the country, close to the French border where myxomatosis was confirmed by August 1953 [19]. This infectious disease then spread in an easterly direction and by the end of 1954 it had spread across the entire country, though the density of confirmed cases in the relatively clayey south of the country was significantly lower than in the more sandier north. This can be explained by the fact that rabbits prefer sandy soils to make their burrows [13], so that larger populations can be expected in the northern part of Belgium.

This infectious disease can be transferred by fleas or mosquitoes that have fed on infected rabbits and by direct contact with infected individuals [5]. Myxomatosis is often lethal for European rabbits [16], and leads to easily observable symptoms, such as skin tumors, fatigue and fever [10].

2.2 The Spatially Explicit Myxomatosis Model

The authors of [3] take the model of Anderson and May [1] as starting point for deriving a non-spatial model of myxomatosis for the European rabbit. The latter model is given by [1]:

$$\begin{cases} \dfrac{dS}{dt} = r\,(S+I+R) - \beta\,S\,I - m\,S\,, \\ \dfrac{dI}{dt} = \beta\,S\,I - (\alpha+m+\nu)\;I\,, \\ \dfrac{dR}{dt} = \nu\,I - m\,R\,, \\ \dfrac{dD}{dt} = m\;(S+I+R) + \alpha\,I\,, \end{cases} \tag{1}$$

where S [–], I [–], R [–] and D [–] represent the number of susceptible, infected, recovered and died individuals, respectively, r [T^{-1}] is the natural per capita birth rate, m [T^{-1}] is the natural per capita death rate, α [T^{-1}] is the additional per capita death rate of infected individuals caused by the disease, β [T^{-1}] is a measure of the contact rate between infected and susceptible individuals, and finally ν [T^{-1}] represents the per capita recovery rate.

As the focus of this paper is on a spatial SA, we do not distinguish between juvenile and adult individuals as in [3], but we take System (1) as starting point to devise a SEM for myxomatosis among European rabbits. More specifically, we conceive the spatial domain as an assembly of irregular polygons c_i as they typically arise in the framework of geographical information science. Besides, we discretize time in the sense that the number of individuals in every health class

is updated in discrete time steps t, each of them corresponding with the same amount of time Δt [T]. The number of susceptible, infected, recovered and died individuals in a polygon c_i at time step t is referred to accordingly as $S(c_i,t)$, $I(c_i,t)$, $R(c_i,t)$ and $D(c_i,t)$, and the spatially explicit counterpart of System (1) can be written as:

$$\begin{cases} S(c_i,t+1) = S(c_i,t) + r\,\Delta t\big(S(c_i,t)+R(c_i,t)\big) - \underline{\beta}\,\Delta t\,S(c_i,t)\,I(c_i,t) - \\ \qquad\qquad \Delta t\,S(c_i,t)\sum\limits_{c_j\in\mathcal{N}_i}\overline{\beta}\,O_{ij}\,I(c_j,t) - m\,\Delta t S(c_i,t) \\ I(c_i,t+1) = I(c_i,t) + \underline{\beta}\,\Delta t\,I(c_i,t)\,S(c_i,t) + \\ \qquad\qquad \Delta t\,S(c_i,t)\sum\limits_{c_j\in\mathcal{N}_i}\overline{\beta}\,O_{ij}\,I(c_j,t) - (\epsilon\gamma + m + \epsilon(1-\gamma))\;\Delta t\,I(c_i,t) \\ R(c_i,t+1) = R(c_i,t) + \epsilon(1-\gamma)\,\Delta t\,I(c_i,t) - m\,\Delta t R(c_i,t) \\ D(c_i,t+1) = D(c_i,t) + m\,\Delta t\big(S(c_i,t)+I(c_i,t)+R(c_i,t)\big) + \epsilon\gamma\,\Delta t\,I(c_i,t) \end{cases} \tag{2}$$

where $\mathcal{N}_i$ is the neighbourhood of polygon c_i that encloses all the polygons surrounding c_i with whose individuals the ones in c_i can interact O_{ij} [−] represents the proportion of c_i's circumference shared with c_j. Here, we will assume that c_i's neighbourhood encloses c_i itself and the polygons with which it shares at least a vertex. Further, $\underline{\beta}$ [T^{-1}] and $\overline{\beta}$ [T^{-1}] denote the short-range and long-range contact rates, respectively, ϵ [T^{-1}] is the reciprocal of the rabbit survival time, and finally, γ [−] is the disease mortality. Essentially, the model given by System (2) is a so-called continuous CA, also known as a coupled-map lattice.

3 Experimental Setup

Based on the average and maximum rabbit densities reported in [21], we assume a density of five individuals per hectare in Belgium. Further, given the fact that myxomatosis was introduced in 1953 through the nidi of infection in the border region between the north of France and Belgium [19], the initial condition was defined in such a way that infected populations were present just across the French side of the border at the end of August 1953. Based on the values reported in [3,21], we further took $r = 9.13 \times 10^{-3}$ d^{-1}, $m = 8 \times 10^{-3}$ d^{-1}, $\epsilon = 0.05$ d^{-1} and $\gamma = 0.8$ d^{-1}. For what concerns the short-range and long-range contact rates, we took the value reported in [3], namely $\underline{\beta} = \overline{\beta} = 2 \times 10^{-3}$ d^{-1}, thereby assuming that the contact rate between individuals living in the same cell is as high as the rate of contact between individuals living in neighbouring cells.

The local SA was performed by perturbing the model parameters one at a time at different points in their biologically meaningful range [3] (Table 1), and tracking the impact on the simulated number of infected individuals as

$$\frac{I(c_i,t) - \widetilde{I}(c_i,t)}{\Delta p}\,, \tag{3}$$

where p denotes an arbitrary parameter, and $\widetilde{I}(c_i, t)$ represents the simulated infected number of individuals if the model is evolved with a perturbed parameter. Further, $\Delta p = \delta p$ with δ a perturbation factor, which was chosen in such a way that the sum of squared errors at consecutive time steps between the finite difference approximation given by Eq. (3) and its backward counterpart was minimal, namely $\delta = 10^{-6}$. So, here we stick to the approach outlined in [23], though the magnitude of the parameter perturbations could be defined in a more natural way if relevant field data are available. Besides, we also kept track of the relative sensitivity, given by

$$p \, \frac{I(c_i, t) - \widetilde{I}(c_i, t)}{\Delta p} \, , \tag{4}$$

because this quantity allows for comparing the model sensitivity with respect to different parameters. Acknowledging the fact that $I(c_i, t)$ depends on both time and space, the computed sensitivities can be aggregated either over time (spatial sensitivity) or over space (temporal sensitivity). Throughout the remainder of this paper, we use the maximum and average operators respectively for this purpose.

Table 1. Parameter ranges and corresponding increments considered for the local SA of System (2)

Parameter	Range	Increment
ϵ	$[0.02, 0.1]$	$10\,10^{-3}$
γ	[0.50,0.99]	$10\,10^{-3}$
r	$2/3\,[0.5/365, 5/365]$	$2/3\,0.25/365$
m	$[6\,10^{-3}, 0.02]$	$0.5\,10^{-3}$
$\underline{\beta}$	$[0.25\,10^{-3}, 0.01]$	$0.25\,10^{-3}$
$\overline{\beta}$	$[0.25\,10^{-3}, 0.01]$	$0.25\,10^{-3}$

All simulations were run in Mathematica (version 10.0.0, Wolfram Research Inc., Champaign, United States) on the high-performance computing infrastructure of Ghent University for 3000 time steps, corresponding with 1500 days as we chose $\Delta t = 0.5$ d.

4 Results

Figure 1 depicts a snapshot of the simulated fraction of infected individuals in the study area after 25 days (September 26, 1953), together with the location of the peak of the epidemic wave at every other 50 days until September 16, 1954. For the sake of comparison, the aforementioned fraction is expressed as the number of infected individuals in a given cell c_i over the maximum number of

living individuals (susceptible, infected and recovered) in any of the cells, i.e. as $I(c_i,t)/\max_j(S(c_j,t)+I(c_j,t)+R(c_j,t))$. This figure unmistakably demonstrates that System (2) gives rise to travelling waves that propagate eastwards from the French-Belgian border where myxomatosis had been confirmed by the end of August 1953. Such waves have been observed for myxomatosis [9], so the present model is definitely capable of a evolving a qualitatively similar dynamics. Moreover, although we leave a sound validation of the presented model for a more comprehensive work, it should be mentioned that the occurrence of the in silico peaks roughly agrees in several seriously affected towns and villages (e.g. Antwerp, Ostend, Bruges, De Panne, ...) with those that were registered in situ [19].

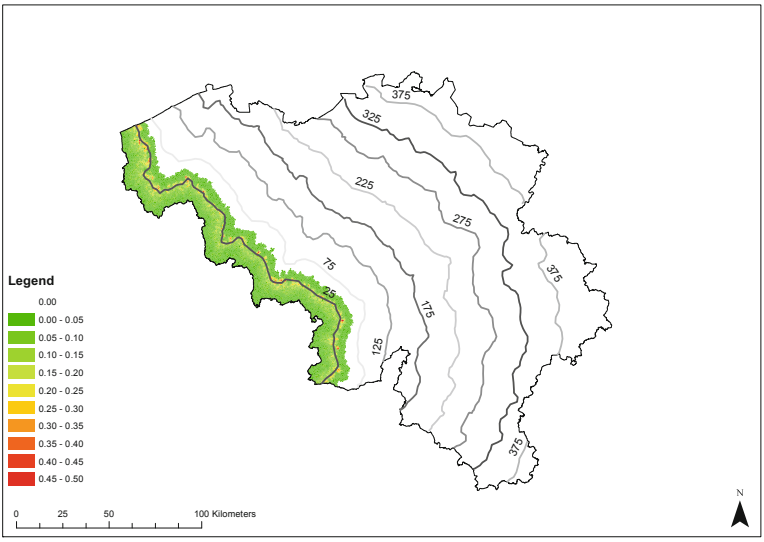

Fig. 1. Simulated proportion of infected individuals in the study area after 25 days (September 26, 1953), and location of the peak of the epidemic wave at every other 50 days until September 16, 1954

The temporal sensitivity of System (2) with respect to ϵ, γ, r and m is given in Fig. 2 for several points in the considered parameter ranges (cfr. Table 1). From the sensitivity plots in this figure it can be inferred that in some cases the magnitude and/or sign of the temporal sensitivity strongly depend(s) on the point in the parameter space that was perturbed, which is a known drawback of local SAs [11]. Still, these plots show that for most of the considered parameter values the temporal sensitivity approaches zero by the end of the simulation period, which can be understood by the fact that the same single steady state is reached, irrespective of the perturbation. It is clear that all parameters have a substantial impact on the simulated dynamics, from which we may conclude that none of them and none of the terms in the model equations are redundant. Still,

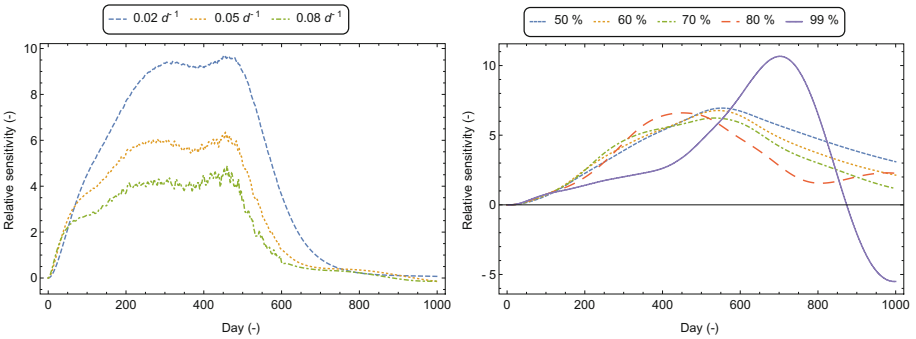

(a) death rate due to the disease (ϵ)

(b) disease mortality (γ)

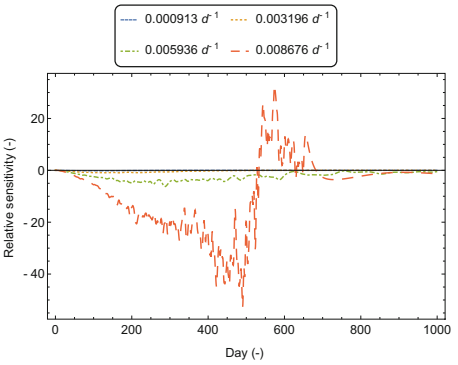

(c) natural birth rate (r)

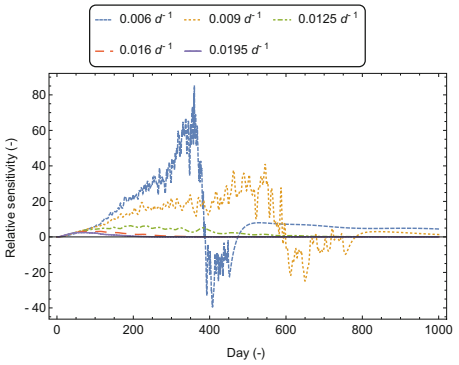

(d) natural death rate (m)

Fig. 2. Temporal sensitivity of System (2) with respect to the death rate due to the disease ϵ (a), the disease mortality γ (b), the natural birth rate r (c) and the natural death rate m (d).

it can be observed that the impact of the death rate due to the disease (ϵ) and the disease mortality (γ) are roughly the same. The effect of the natural death rate (m) and the natural birth rate (r) is for most of the considered parameter values less pronounced, even though the latter parameters can lead to the highest relative sensitivity values among the ones observed for the studied parameters. From Fig. 2(a) we further infer that a slight increase of the death rate due to the disease ϵ negatively affects the number of infected individuals, and that this effect is more pronounced as ϵ is lower. Although this seems contradictory at first, this can be understood by acknowledging that also the amount of available time for transmitting the disease decreases as ϵ increases, and so the rabbit survival time ϵ^{-1} decreases. A similar reasoning can be followed to understand the temporal sensitivity of System (2) with respect to the mortality rate γ, though this one can be come negative in the long run if evaluated for very high γ (e.g. $\gamma = 99\,\%$). On the other hand, a slight increase of the natural birth rate r leads to an increase in the number of infected individuals, and this effect becomes more pronounced

as the perturbed parameter value is higher. Yet, when r is already very high (i.e. $r = 8.676$ d^{-}1), the opposite is true from a certain moment in time on. This tipping point occurs when the epidemic wave has covered the entire country, and rabbit populations countrywide can (partly) recover.

The spatial sensitivity of System (2) with respect to $\overline{\beta} = 5\,10^{-3}\,\mathrm{d}^{-1}$ is depicted in Fig. 3. Despite all model parameters are spatially homogeneous, the spatial sensitivity strongly depends on the location. Not only does the sensitivity increase with increasing distance from the source of infection (the border between France and Northwest of Belgium), as could have been anticipated, but regions at a similar distance from this source can have a completely different spatial sensitivity. This information cannot be derived from a classical SA, and it is to be expected that the spatial heterogeneity of the model sensitivity would increase even further when some of the model inputs and/or parameters would vary spatially.

This demonstrates that a SA of any SEM should be performed comprehensively so that it allows to investigate the sensitivity both from a temporal and a spatial point of view. In this way, one can identify the regions where the simulation results are still relatively reliable in the case of uncertain/imprecise model parameters and it allows to understand how sensitivity varies spatially both in terms of its magnitude and sign. A more comprehensive SA should, however, consist of both a global and local SA, where the former will allow to identify the most influential model parameter, whose effect can subsequently be analysed by conducting a local SA.

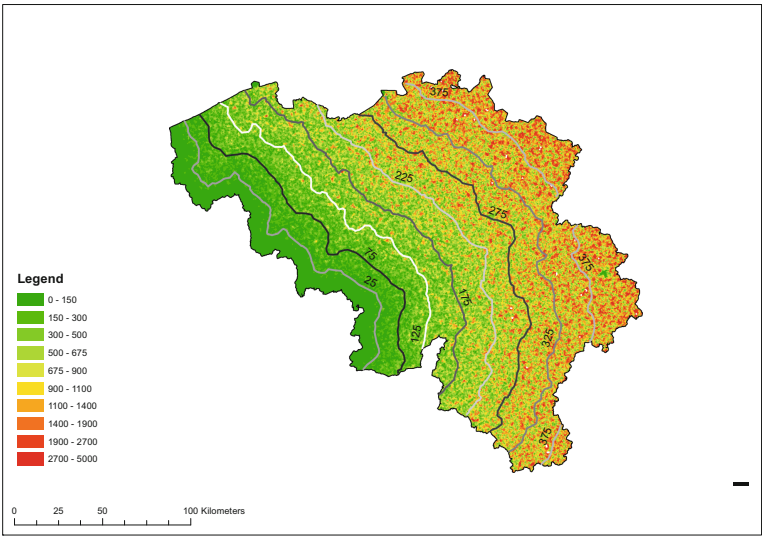

Fig. 3. Spatial sensitivity of System (2) with respect to the long-range contact rate $\overline{\beta} = 5\,10^{-3}\,\mathrm{d}^{-1}$.

Acknowledgements. This work was carried out using the STEVIN Supercomputer Infrastructure at Ghent University, funded by Ghent University, the Flemish Supercomputer Center (VSC), the Hercules Foundation and the Flemish Government.

References

1. Anderson, R.M., May, R.M.: Population biology of infectious diseases: Part 1. Nature **280**, 361–367 (1979)
2. Chitnis, N., Hyman, J.M., Cushing, J.M.: Determining important parameters in the spread of malaria through the sensitivity analysis of a mathematical model. Bull. Math. Biol. **70**, 1272–1296 (2008)
3. Dwyer, G., Levin, S.A., Buttel, L.: A simulation model of the population dynamics and evolution of myxomatosis. Ecol. Monogr. **60**, 423–447 (1990)
4. Fenner, F., Fantini, B.: The discovery of myxoma virus. In: Fenner, F., Fantini, B. (eds.) Biological Control of Vertebrate Pests: The History of Myxomatosis, an Experiment in Evolution, pp. 65–92. CABI Publishing, Wallingford, United Kingdom (1999)
5. Fenner, F., Ross, J.: The European Rabbit: The History and Biology of a Successful Colonizer. Oxford University Press, Oxford (1994)
6. Fisher, P., Abrahart, R.J., Herbinger, W.: The sensitivity of two distributed non-point source pollution models to the spatial arrangement of the landscape. Hydrol. Process. **11**, 241–252 (1997)
7. Frey, H.C., Patil, S.R.: Identification and review of sensitivity analysis methods. Risk Anal. **22**, 553–578 (2002)
8. Grimm, V., Railsback, S.F.: Individual-Based Modeling and Ecology. Princeton University Press, Princeton (2005)
9. Joubert, L., Leftheriotis, E., Mouchet, J.: La Myxomatose. L'Expansion Scientifique Française, Paris (1972)
10. Kritas, S., Dovas, C., Fortomaris, P., Petridou, E., Farsang, A., Koptopoulos, G.: A pathogenic myxoma virus in vaccinated and non-vaccinated commercial rabbits. Res. Vet. Sci. **85**, 622–624 (2008)
11. Ligmann-Zielinska, A., Jankowski, P.: Spatially-explicit integrated uncertainty and sensitivity analysis of criteria weights in multicriteria land suitability evaluation. Environ. Model. Softw. **57**, 235–247 (2014)
12. Lilburne, L., Tarantola, S.: Sensitivity analysis of spatial models. Int. J. Geogr. Inf. Sci. **23**, 151–168 (2009)
13. Lombardi, L., Fernández, N., Moreno, S., Villafuerte, R.: Habitat-related differences in rabbit (oryctolagus cuniculus) abundance, distribution, and activity. J. Mammal. **84**, 26–36 (2003). American Society of Mammalogists
14. Marano, N., Arguin, P.M., Pappaioanou, M.: Impact of globalization and animal trade on infectious disease ecology. Emerg. Infect. Dis. **13**, 1807–1809 (2007)
15. Marcot, B.G., Singleton, P.H., Schumaker, N.H.: Analysis of sensitivity and uncertainty in an individual-based model of a threatened wildlife species. Nat. Resour. Model. **28**, 37–58 (2015)
16. Marlier, D., Mainil, J., Sulon, J., Beckers, J.F., Linden, A., Vindevogel, H.: Study of the virulence of five strains of amyxomatous myxoma virus in crossbred New Zealand white/Californian conventional rabbits, with evidence of long-term testicular infection in recovered animals. J. Comp. Pathol. **122**, 101–113 (2008)

17. Massada, A.B., Carmel, Y., Koniak, G., Noy-Meir, I.: The effects of disturbance based management on the dynamics of mediterranean vegetation: A hierarchical and spatially explicit modeling approach. Ecol. Model. **220**, 2525–2535 (2009)
18. McLeod, R.G., Brewster, J.F., Gumel, A.B., Slonowsky, D.A.: Sensitivity and uncertainty analyses for a SARS model with time-varying inputs and outputs. Math. Biosci. Eng. **3**, 527–544 (2006)
19. Ministère de l'Agriculture: Service Vétérinaire: Bulletin sanitaire. Ministère de l'Agriculture, Service Vétérinaire, Brussels, Belgium (1953)
20. Rinaldi, P.R., Dalponte, D.D., Vénere, M.J., Clausse, A.: Cellular automata algorithm for simulation of surface flows in large plains. Simul. Model. Pract. Theory **15**, 315–327 (2007)
21. Lumpkin, S., Seidensticker, J.: Rabbits: The Animal Answer Guide. Johns Hopkins University Press, Baltimore (2011)
22. Saint-Geours, N., Lavergne, C., Bailly, J., Grelot, F.: Change of support in spatial variance-based sensitivity analysis. Math. Geosci. **44**, 945–958 (2012)
23. Saltelli, A., Chan, K., Scott, E.M.: Sensitivity Analysis. Wiley, West Sussex (2000)
24. Saltelli, A., Ratto, M., Andres, T., Campolongo, F., Cariboni, J., Gatelli, D., Saisana, M., Tarantola, S. (eds.): Global Sensitivty Analysis: The Primer. Wiley, Chichester (2008)
25. Saltelli, A.: Making best use of model evaluations to compute sensitivity indices. Comput. Phys. Commun. **145**, 280–297 (2002)
26. Sobol, I.M.: On sensitivity estimates for nonlinear mathematical models. Matematicheskoe Modelirovanie **2**, 112–118 (1990)
27. Tang, W., Jia, M.: Global sensitivity analysis of a large agent-based model of spatial opinion exchange: A heterogeneous multi-GPU acceleration approach. Ann. Assoc. Am. Geogr. **104**, 485–509 (2014)
28. Tarantola, S., Nardo, M., Saisana, M., Gatelli, D.: A new estimator for sensitivity analysis of model output: An application to the e-business readiness composite indicator. Reliab. Eng. Syst. Saf. **91**, 1135–1141 (2006)
29. von Neumann, J.: The general and logical theory of automata. In: Jeffres, L.A. (ed.) The Hixon Symposium on Cerebral Mechanisms in Behaviour, pp. 1–41. Wiley, Pasadena (1951)
30. Walsh, S., Brown, D.G., Bian, L., Allen, T.R.: Effects of spatial scale on data certainty: An assessment through data dependency and sensitivity analyses. In: Proceedings of the First International Symposium on the Spatial Accuracy of Natural Resource Data Bases, pp. 151–160. American Society for Photogrammetry and Remote Sensing (1994)
31. Wu, J., Dhingra, R., Gambhir, M., Remais, J.V.: Sensitivity analysis of infectious disease models: methods, advances and their application. J. R. Soc. Interface **10**, 20121018 (2013)